Ratio of the surface-enhanced anti-Stokes scattering to the surface-enhanced Stokes-Raman scattering for molecules adsorbed on a silver electrode

A. G. Brolo,[1,*] A. C. Sanderson,[2] and A. P. Smith[1]
[1]*Department of Chemistry, University of Victoria, P.O. Box 3065, Victoria, British Columbia, Canada V8W 3V6*
[2]*Department of Physics and Astronomy, University of Victoria, P.O. Box 3055, Victoria, British Columbia, Canada V8W 3P6*
(Received 20 December 2002; revised manuscript received 15 July 2003; published 30 January 2004)

Surface-enhanced Raman scattering (SERS) from oxazine 720 (oxa), rhodamine 6G (R6G), and pyridine (py) adsorbed on a rough silver surface was observed. The silver electrode was immersed in aqueous solutions permitting control of the potential bias applied to the surface. SERS spectra in the Stokes and anti-Stokes regions were obtained for several applied potentials and two laser excitation energies. Normalized ratios between the anti-Stokes and the Stokes intensities K were calculated from the SERS spectra. The K ratios differed from unity for all the systems investigated. A preferential enhancement of the (surface-enhanced) Stokes scattering was observed for oxa and py. In contrast, the K ratios were higher than unity for R6G, indicating an increase in the anti-Stokes signal. The K ratios measured in this work decreased with the excitation energy and showed a dependence on the energy of the vibrational modes. These results were satisfactorily explained using resonance models, based on the charge-transfer and electromagnetic theories for SERS. No evidence for a SERS-induced nonthermal population distribution among the vibrational states of the adsorbed molecules (vibrational optical pumping) was found. Therefore, we conclude that the main features of the preferential enhancement of the anti-Stokes scattering for an adsorbed molecule on rough silver can be fully understood in the context of current SERS theories.

DOI: 10.1103/PhysRevB.69.045424 PACS number(s): 78.30.−j, 82.45.−h, 78.68.+m, 33.20.Fb

I. INTRODUCTION

The first reports of single-molecule detection (SMD) by surface-enhanced Raman scattering[1,2] (SERS) induced a fast-paced increase in interest in this technique. The physical nature of the ca. 10^{15}-fold enhancement of the Raman cross section intrigued theoreticians,[3] and the potential benefits from the unprecedented combination of sensitivity and specificity were easily foreseen by the analytical chemistry community.[4] These initial results were soon confirmed by several groups.[5–9] It is important to mention that extremely large Raman cross sections from rhodamine 6G (R6G) adsorbed on Ag colloids, although not in the SMD context, had been measured several years earlier.[10,11] SMD-SERS has been observed not only from dyes,[4] but also from biologically relevant molecules, such as DNA bases,[12] proteins,[6] and enzymes.[13] Single molecules of analytes were detected and imaged even in the presence of complex SERS-inactive matrices prepared using the Langmuir-Blodgett technique.[8,14]

At first glance, the exceptional enhancement of the Raman-scattering cross section seemed to be a completely new phenomenon. However, a careful analysis of the reported data indicated that even the most unusual properties attributed to SMD-SERS (such as ''blinking''[15]) could be explained using the accepted SERS theories.[5,9,16] In fact, electromagnetic[3,17,18] (EM) and charge-transfer[5,19,20] (CT) models have been put forward to explain the salient features of the SMD-SERS. According to the EM theory for SERS, the surface enhancement is a result of the excitation of surface-plasmon oscillations by the incident and the scattered fields.[21] The confinement of these oscillations in a specific nanometric-sized region between metallic particles (hot sites) produces a resonance which provides huge and highly localized electromagnetic fields.[3] This effect alone may account for enhancement factors for the Raman cross section ranging from 10^{10} to 10^{12}. The 10^3–10^5 contribution to the total surface enhancement not accounted for by the EM theory can then be attributed to CT effects.[20,22] The most favored CT model is based on the interaction between hot (ballistic) electrons and the adsorbed molecule, as proposed by Otto[23] and Persson.[24] This model also considers a molecule located at the junction between two nanometric SERS-active particles. In this case, however, the plasmon excitation is manifested in terms of electron-hole resonances. The charged carriers can then hop between particles using a molecular orbital bridge, creating optical currents that can sustain significant enhancement of the Raman signal.[5,19,20]

Despite the wealth of both theoretical and experimental information generated in recent years, one phenomenon linked to the enormous Raman cross section responsible for the SMD-SERS still remains controversial: the preferential enhancement of the anti-Stokes scattering observed for dyes adsorbed on silver colloids.[25,26] Kneipp and co-workers[26] measured the ratio between the intensity of the surface-enhanced anti-Stokes and surface-enhanced Stokes scattering $[(I_{AS}/I_S)_{SERS}]$ for several dyes. The $[(I_{AS}/I_S)_{SERS}]$ ratio was normalized to the anti-Stokes to Stokes ratio from an unenhanced Raman (UR) scatterer in solution $[(I_{AS}/I_S)_{UR}]$, according to[26]

$$K=\frac{\left(\frac{I_{AS}}{I_S}\right)_{SERS}}{\left(\frac{I_{AS}}{I_S}\right)_{UR}}. \tag{1}$$

The ratio K was significantly higher than 1 for all dyes

investigated, indicating a preferential increase in the intensity of the anti-Stokes scattering.[26] The *K* ratios were also found to increase significantly with the vibrational wave number.[26] A quadratic dependence of intensity of the surface-enhanced anti-Stokes scattering on the incident laser power was also demonstrated.[26] These features were attributed to strong optical pumping to vibrationally excited states, induced by the large SERS enhancement experienced by a small number of molecules.[26] According to Ref. 26 a large photon density of the excitation radiation combined with the exceptional surface-enhanced Raman cross section should significantly populate the first vibrationally excited state of a given vibrational mode (assuming a vibrational relaxation of the order of 10 ps). This effect would lead to a nonthermal overpopulation of higher vibrational states and an increase in the intensity of the anti-Stokes scattering from what would be expected from a system with a Boltzmann distribution.

A method for the determination of effective SERS cross section of biologically relevant molecules was developed using the optical pumping concept.[12] It was also recently suggested that strong surface-enhanced anti-Stokes scattering could be used as a new incoherent two-photon Raman probe with useful biophysical applications.[27]

The above unity *K* ratios were reproduced by Haslett *et al.*[25] for rhodamine 6G (R6G) and crystal violet adsorbed on silver colloidal particles. These authors observed *K* ratios close to unity for colorless molecules, such as pyridine and phthalazine, adsorbed on the same type of substrates.[25] Moreover, a linear dependence of the Raman intensities with the incident laser power was reported[25] rather than a quadratic one.[26] Although in close agreement with most of the experimental features presented in Ref. 26, Haslett *et al.* challenged the optical pumping model suggested by Kneipp *et al.* to explain the nonunity *K* ratios.[25] According to the EM mechanism, the incident field enhanced by the resonant interaction with surface-plasmon oscillations accounts for only part of the total enhancement.[21] An equally important contribution to the total EM enhancement originates from the resonance of the surface plasmon with the scattered field generated by the molecule.[21] This latter contribution yields Raman photons from the metal substrate and thus should not be involved in optical pumping. Therefore, for SERS-induced optical pumping, the resulting nonequilibrium situation must be driven solely by the incident field. Consequently, it was easily demonstrated by Haslett *et al.*[25] that the predicted field intensity to allow optical pumping through the mechanism proposed in Ref. 26 would be prohibitively high (ca. 10^{15} W cm^{-2}). These tremendous fields should provoke significant ionization and molecular decomposition. Since no support for optical pumping was found, the resulting *K* ratios were assigned to differences in the cross sections for the surface-enhanced Stokes and anti-Stokes scattering caused by a resonant silver-adsorbate CT complex.[25]

Electrochemical SERS may be a good experimental approach to the solution of this controversy. The CT contribution to the enhancement can be verified under electrochemical conditions since the dependence of the intensities of the SERS bands with the electric potential bias applied to the metal surface is related to CT resonances.[28] In the present work, we measured the electrochemical SERS spectra of R6G, oxazine 720 (oxa), and pyridine (py) adsorbed on a silver electrode. The electric field at the silver-aqueous solution interface was varied and two excitation energies were used. Surface-enhanced Stokes and surface-enhanced anti-Stokes scattering intensities were measured for several different conditions. Moreover, these experiments were not performed under conditions that would allow optical pumping as established in Ref. 26 (high laser power density and enormous SERS cross section seem to be among the main requirements for optical pumping according to Ref. 26). Therefore, under our experimental conditions, with incident power densities orders of magnitude lower than in Ref. 26, optical pumping should not be responsible for *K* ratios different than unity.

II. EXPERIMENT

A. Solutions

The following chemicals were used without further purification: KCl (ACP), $NaClO_4$ (ACP), pyridine (Aldrich), oxazine 720 (Lambda), and rhodamine 6G (Lambda). All solutions were prepared using ultrapure water (18.2 MΩ) from a Barnstead NANOpure Diamond water purification system.

B. Cell, electrodes, and electrochemical equipment

The working electrode was fabricated using a 99.99% silver rod (Premion—Alfa Aesar). A silver disk of ca 6.35 mm diameter was mounted in a Teflon holder. Electrical contact was made to the silver electrode by an externally threaded stainless-steel rod. The silver electrode was polished before each experiment with emery paper and then with progressively finer grades of alumina powder down to 0.05 μm. After the surface polishing treatment, the silver electrode was rinsed with copious amounts of ultrapure water and then transferred to the appropriate cell. A saturated silver/silver chloride electrode was used as reference, and all potentials in this work are quoted against this reference. A 0.3 mm platinum wire (Alfa Aesar) was used as the counterelectrode. The spectroelectrochemical cell used for SERS measurements has been described in a previous publication.[28] A Hokuto Denko potentiostat-galvanostat (HAB-151) was used to control the potential bias applied to the silver surface. The assembled cell was purged with prepurified N_2 for 30 min prior to the measurements, and a gentle stream of nitrogen was maintained to blanket the solution during data acquisition.

C. Activation procedure

A rough surface is required for the observation of SERS.[28] The electrochemical protocol used to generate the necessary roughness is referred to as the ''activation procedure.'' The activation procedure used in this work consists of a sequence of oxidation-reduction cycles (ORC's) performed on the polished silver electrode immersed in an aqueous solution containing 0.2 M KCl. The potential of the silver-solution interface was initially held at -700 mV. A triangular potential sweep program was then applied, changing the surface potential from its initial value to an upper limit of $+250$ mV

before returning to −700 mV. The scan rate used during this treatment was 5 mV s^{-1}. Typically, three such cycles were performed to produce the desired roughness. The metallic silver oxidizes in this medium at potentials more positive than +50 mV. The oxidation product is an insoluble salt (AgCl) that accumulates at the surface during the forward scan. In the reverse scan, however, the AgCl film is reduced back to metallic silver when the applied bias is equal to ca. −100 mV. The freshly formed silver surface obtained during the reduction is naturally rough, with features ranging from 50–400 nm in size.[29,30] This type of surface facilitates significant enhancement of the Raman signal for adsorbed molecules.[28,30]

Several protocols were used to add the organic molecule to the activated silver surface. For py, the applied potential was held during the reverse portion of the potential cycle immediately after the reduction of the silver chloride, and the organic molecule was added to the solution in the cell to produce the desired final concentration. Another procedure consisted of activating the electrode followed by removing it to ambient atmosphere and adding a drop of a low concentration solution of the dye in methanol to the electrode surface. The solvent was then removed by evaporation, after which the surface was rinsed with ultrapure water. The modified electrode surface (with the organic molecule now adsorbed on it) was then placed back into the cell. The electrochemical control was resumed and the desired potential bias was applied. This procedure ensures that at most 1 ML of the dye stays adsorbed on the surface. The high quality of the SERS spectra obtained from both R6G and oxa adsorbed using this procedure indicates that an extremely large enhancement of the Raman cross section was obtained for these molecules.

SERS experiments were also performed in 0.1 M $NaClO_4$ solutions instead of 0.2 M KCl. Although changes in solution yield different SERS enhancement factors, they do not significantly affect the ratio between the Stokes and anti-Stokes scattering intensities. The silver electrode was never oxidized in the presence of the molecule of interest. This ensured that the organic molecule was neither trapped nor electrochemically degraded by the activation ORC.[31]

D. Raman instrumentation

Raman spectra were collected using a Dilor OMARS89 spectrometer coupled to an optical multichannel analyzer. The detector was a thermoelectrically cooled (ca. −15°C) intensified diode array (512 diodes). The spectrometer was interfaced to a computer for data collection. Excitation at 514.5 nm was provided by a Spectra Physics Model 2020 argon-ion laser. A Melles Griot He-Ne laser was used as the 632.8 nm excitation source. Both lasers supplied less than 20 mW to the sample. The acquisition time for each measurement was 1 s and a minimum of ten accumulations were summed for each spectrum. The laser light was chopped to allow background spectra to be obtained and subtracted during each accumulation. The resulting spectra were then base line corrected during analysis.

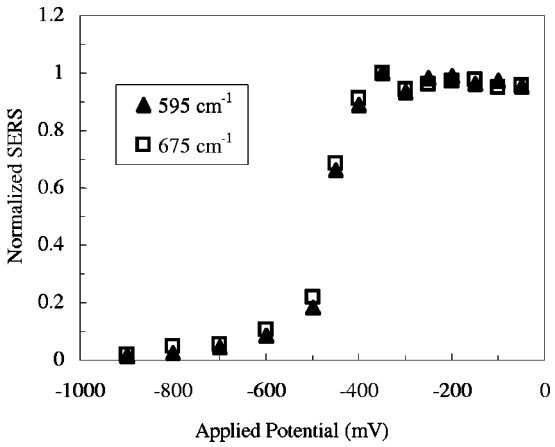

FIG. 1. Potential profiles of the 595 cm^{-1} and 675 cm^{-1} vibration bands of oxazine 720 adsorbed on a roughened silver electrode. Excitation is provided by the 514.5 nm Ar^+ line.

III. RESULTS AND DISCUSSION

Prominent peaks at 544, 584, 672, 1335, 1393, and 1638 cm^{-1} were observed from oxa adsorbed on silver. Although there are no previous reports in the literature dealing with electrochemical SERS of oxa, the SERS spectra from oxa adsorbed on a roughened silver electrode obtained in this work present several similarities to the SERS spectra of oxa adsorbed on silver colloids reported by Schneider *et al.*[32] Some discrepancies were noted between the relative intensities of the SERS spectra we observed and the ones reported in Ref. 32. These can be ascribed to differences in the morphology of the SERS substrates and to effects of the applied potential.

The normalized intensity of the vibrational SERS bands from oxa adsorbed on silver was plotted against the applied potential bias. This type of curve is referred to throughout this paper as a potential profile. Figure 1 shows potential profiles for the surface-enhanced Stokes bands at 595 and 675 cm^{-1} for oxa adsorbed on a roughened silver electrode obtained using a laser excitation at 514.5 nm (ca. 19 436 cm^{-1} or 2.41 eV). The SERS bands of oxa adsorbed on silver present maximum intensities when the electric potential applied to the surface is between −50 and −450 mV. The SERS signal drops sharply between −450 and −600 mV and decreases further as the potential is made more negative (Fig. 1). The behavior presented in Fig. 1 suggests that an electron is transferred to the molecule between −450 and −600 mV. The SERS signal reaches a minimum at the extreme negative limit in Fig. 1 but it is fully recovered when the applied potential bias is stepped back to more positive values (for instance, from −900 to −100 mV). This indicates that the suggested electron-transfer process is reversible. The value of the potential where this charge-transfer occurs (ca −500 mV) is consistent with a low-lying lowest unoccupied molecular orbital for this molecule. The main characteristics of the potential profile presented in Fig. 1 were reproduced in experiments using 632.8 nm (ca 15803 cm^{-1} or 1.96 eV) laser excitation.

The characteristic SERS vibrational bands for R6G adsorbed on a silver electrode observed at ca 620, 770, and

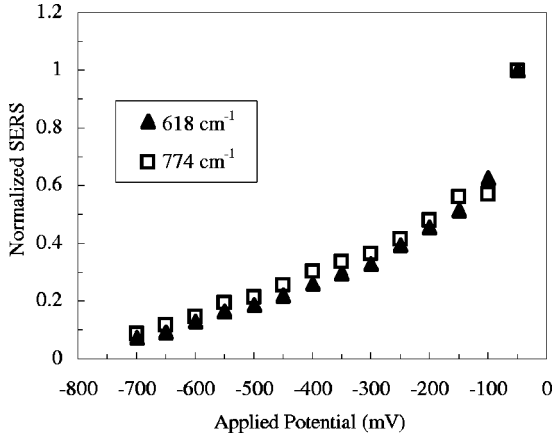

FIG. 2. Potential profiles of the 618 cm^{-1} and 774 cm^{-1} vibration bands of rhodamine 6G adsorbed on a roughened silver electrode. Excitation is provided by the 632.8 nm He-Ne line.

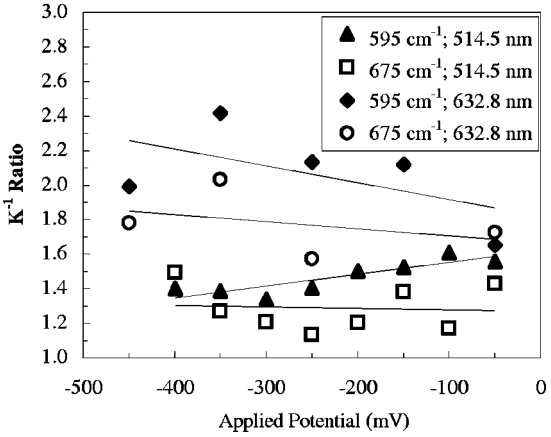

FIG. 4. K^{-1} ratios of the 595 cm^{-1} and 675 cm^{-1} vibration bands of oxazine 720 adsorbed on a roughened silver electrode excited by the 514.5 nm Ar^{+} and 632.8 nm He-Ne lines.

1180 cm^{-1} agree well with results available in the literature.[10,11,25,26,33] The potential profiles for the surface-enhanced Stokes bands of R6G at ca. 620 and 1180 cm^{-1}, obtained using 632.8 nm excitation, are presented in Fig. 2. The maximum SERS intensity for both bands is observed at the most positive potential. The SERS signal in Fig. 2 decreases as the potential bias is made more negative, as observed in Fig. 1. However, Fig. 1 shows a quasiconstant maximum intensity over a large potential range followed by a sudden drop, whereas the decrease in SERS intensity with potential is less pronounced in Fig. 2. There is no clear indication of electron transfer for R6G and no reversible recovery of the SERS signal when the potential is stepped from the negative limit to a more positive potential.

The SERS of py adsorbed on a silver surface under electrochemical control presents strong vibrational bands at 632, 1002, 1032, 1220, and 1596 cm^{-1}. These general features agree well with available literature for pyridine adsorbed on silver,[34–36] gold,[37] and copper[38] electrodes. Figure 3 shows the potential profile for the ring breathing band of py at 1003 cm^{-1} for two excitation energies. Each excitation yields a bell shaped curve with maximum intensity at a specific applied potential Φ_{max}. This curve is in contrast with those of the dyes presented in Figs. 1 and 2. Φ_{max} for the py curve in Fig. 3 is about -600 mV with the green excitation (514.5 nm), but is shifted to ca -850 mV for the red excitation (632.8 nm).

The potential profiles obtained from oxa, R6G, and py adsorbed on a roughened silver surface (including those presented in Figs. 1–3) for both the Stokes and anti-Stokes scattering were used to calculate K ratios. The UR spectra of pure liquid benzene and carbontetrachloride were measured and used in the ratio calculation according to Eq. (1). This procedure compensates for differential instrument response in the Stokes and anti-Stokes regions. Figure 4 shows K^{-1} ratios for oxa plotted versus the applied potential bias for two distinct excitation wavelengths (514.5 nm and 632.8 nm). Figure 5 shows a similar plot using the SERS data obtained from py. Notice that K^{-1} is a more convenient (and meaningful) quantity than K in these cases (Figs. 4 and 5). Although a slight slope is present, the maximum variation in the ratio is less than ± 1 over the range of potentials applied.

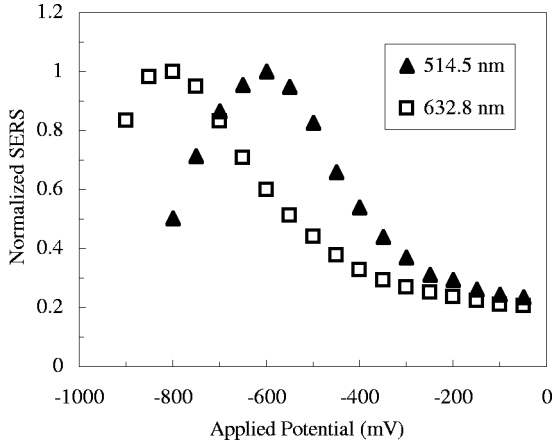

FIG. 3. Potential profile of the 1003 cm^{-1} vibration band of pyridine adsorbed on a roughened silver electrode excited by the 514.5 nm Ar^{+} and 632.8 nm He-Ne lines.

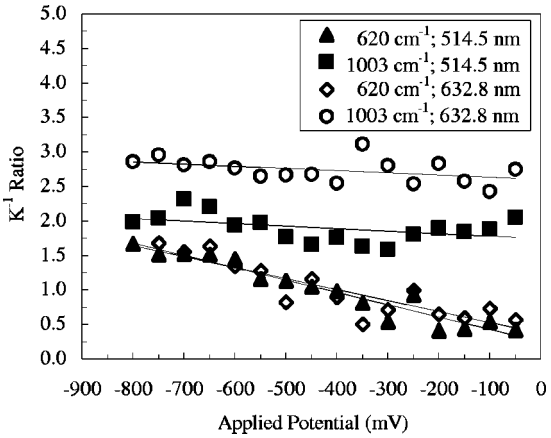

FIG. 5. K^{-1} ratios of the 620 cm^{-1} and 1003 cm^{-1} vibration bands of pyridine adsorbed on a roughened silver electrode excited by the 514.5 nm Ar^{+} and 632.8 nm He-Ne lines.

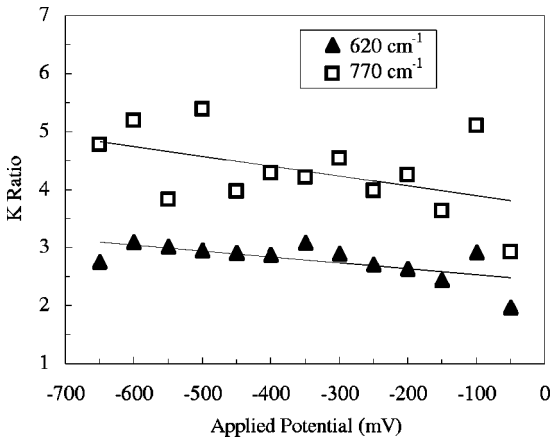

FIG. 6. *K* ratios of the 620 cm^{-1} and 770 cm^{-1} vibration bands of rhodamine 6G adsorbed on a roughened silver electrode excited by the 632.8 nm He-Ne line.

It is important to mention that the error on the experimentally calculated ratios using Eq. (1) typically increases with the energy of the vibrational mode since the absolute anti-Stokes Raman signal decreases with energy, causing an increase in the statistical uncertainty. The absolute intensities of the SERS bands of oxa and R6G decrease at negative potentials, causing additional uncertainty in the calculated *K* ratios. This explains some of the fluctuations observed in Figs. 4–6.

For oxa (Fig. 4) the K^{-1} ratios for the bands at ca. 595 and 675 cm^{-1} are between 1.2 and 1.5 with the green excitation (514.5 nm) and between 1.8 and 2.2 with the red excitation (632.8 nm). For a given excitation energy, the K^{-1} ratios for the two bands are very similar. The results obtained for pyridine adsorbed on a silver electrode, presented in Fig. 5, indicate K^{-1} ratios of ca 1 for the 620 cm^{-1} band for both green and red excitations. The K^{-1} ratios for the ring breathing mode (1003 cm^{-1}) were found to be around 1.8 and 3.0 for green and red excitations, respectively. The K^{-1} ratios higher than unity observed in Figs. 4 and 5 indicate a preferential increase of the surface-enhanced Stokes scattering relative to the surface-enhanced anti-Stokes scattering.

Figure 6 shows a plot of the *K* ratios for different bands of R6G at several applied potentials using 632.8 nm excitation. Attempts to measure the SERS of R6G using 514.5 nm were unsuccessful due to fluorescence and photodecomposition. *K* ratios between 2.5 and 3.0 and between 3.5 and 5.5 were obtained for the bands at 620 and 770 cm^{-1}, respectively. Therefore, the *K* ratios in Fig. 6 increase with the vibrational energy for a given applied potential. However, *K* ratios higher than unity were observed for all vibrational bands of R6G adsorbed on a silver electrode. The *K* ratios higher than 1 indicate that a relative enhancement of the anti-Stokes scattering occurred, as observed in Ref. 25 and 26.

K^{-1} ratios for the SERS of pyridine adsorbed on Cu, Ag, and Au were obtained by others using several excitation wavelengths.[39] Marinyuk *et al.*[39] reported K^{-1} ratios higher than 1 for all excitation energies. This is in good agreement with the results for py presented in Fig. 5. However, a higher K^{-1} ratio was observed in Ref. 39 for 514.5 nm excitation than for 632.8 nm and their K^{-1} ratios were potential independent.

Several factors may contribute to the dependence of the SERS intensities on the applied potential bias presented in Figs. 1–3. These contributions may include electrochemical reaction (electron transfer between the metal and the adsorbate as observed for oxa in Fig. 1), molecular reorientation and changes in the amount of adsorbed species with the applied potential. No potential-induced reorientation was observed for any of the molecules investigated in this work, as evidenced by the consistency of the spectral features as the applied potential was varied. The two dye species, oxa and R6G produce a maximum SERS intensity at the most positive potentials, which decreases as the applied potential is made more negative (Figs. 1 and 2). This type of potential dependence is observed for both excitation energies. Moreover, the potential where the SERS signal is maximum (Φ_{max}) is dependent on the excitation wavelength for py (Fig. 3). The behavior observed in Figs. 1–3 can be interpreted as a manifestation of the CT contributions to the overall enhancement.[40,41]

Resonance arguments can also be invoked to explain the results presented in Figs. 4–6. If formation of metal-adsorbate charge-transfer complexes is assumed for each of the molecules investigated in this work, the preferential enhancement of either the Stokes (Figs. 4 and 5) or the anti-Stokes (Fig. 6) scattering must be assigned to the relative position of the absolute energy of the Raman-shifted photon to the electronic transition of the complex. This type of situation is common in the resonance Raman literature, and the *K* ratios can be readily calculated using[39,42]

$$K=\left(\frac{(\overline{\nu}_{exc}+\overline{\nu}_{vib})^3_{SERS}(\overline{\nu}_{exc}-\overline{\nu}'_{vib})^3_{UR}}{(\overline{\nu}_{exc}-\overline{\nu}_{vib})^3_{SERS}(\overline{\nu}_{exc}+\overline{\nu}'_{vib})^3_{UR}}\right)\exp\left(-\frac{\overline{\nu}_{vib}}{kT_{SERS}}\right)$$
$$\times\exp\left(\frac{\overline{\nu}'_{vib}}{kT_{UR}}\right)\left(\frac{(\overline{\nu}_{exc}-\overline{\nu}_{elect}-\overline{\nu}_{vib})^2+\Gamma^2}{(\overline{\nu}_{exc}-\overline{\nu}_{elect}+\overline{\nu}_{vib})^2+\Gamma^2}\right). \quad (2)$$

The subscripts SERS and UR correspond to the adsorbed molecule and the pure liquid used as a reference, as in Eq. (1), respectively. The energies (in cm^{-1}) for the excitation laser, the vibrational mode of the SERS band, the vibrational mode of the UR band, and the electronic transition of the complex are $\overline{\nu}_{exc}$, $\overline{\nu}_{vib}$, $\overline{\nu}'_{vib}$, and $\overline{\nu}_{elect}$, respectively. Temperatures are designated by *T* and *k* is the Boltzmann constant (in cm^{-1}). A damping factor (in cm^{-1}) Γ is related to the half-width of the electronic band of the complex. It should be noted that Eq. (2) was formulated under the assumption that the nonresonance part of the Raman tensor responsible for a given Stokes scattering is equal to its anti-Stokes counterpart, allowing their ratio to be eliminated from the equation. Equation (2) is further simplified with the following assumptions. The same vibrational energy can be assumed for both the SERS and the reference ($\overline{\nu}_{vib}=\overline{\nu}'_{vib}$), which can be achieved by careful selection of the reference material. The exponential terms can also be canceled out by

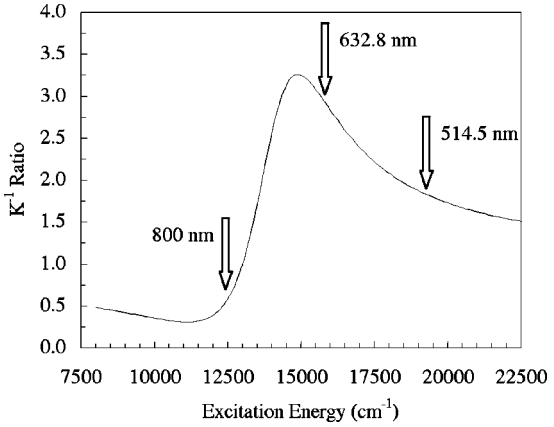

FIG. 7. Dependence of K^{-1} on the excitation energy used in a resonance Raman model with $\bar{\nu}_{\mathrm{elec}}=13\,300\ \mathrm{cm}^{-1}$ and $\Gamma=1600\ \mathrm{cm}^{-1}$. The arrows are at typical laser excitations: Ti-sapphire at 800 nm, He-Ne at 632.8 nm, and Ar^+ at 514.5 nm.

considering the same temperature at the surface and in the reference liquid ($T_{\mathrm{SERS}}=T_{\mathrm{UR}}$). With these approximations only the last term on the right-hand side of Eq. (2) (the term in parentheses after the exponentials) should contribute to the total K ratio.

Figure 7 shows a plot of the inverse of Eq. (2) (K^{-1}), at different excitation energies using all the approximations mentioned above, for a vibrational mode at 1000 cm^{-1}. This vibrational energy is similar to the observed ring breathing vibration of adsorbed py. The energy of the electronic transition and the value for the half-width of the electronic band were adjusted to match the K^{-1} ratios observed in Fig. 5 for the ring breathing mode (1003 cm^{-1}) of py adsorbed on silver. It is important to point out, however, that the objective was not to fit the equation to our experimental value to extract the electronic transition parameters. This would not yield a satisfactory result, since more than one $\bar{\nu}_{\mathrm{elec}}$ and Γ combination would reproduce our limited number of data points (our experiments were realized using only two excitation energies). The goal here is to demonstrate that the experimental results presented in Figs. 4–6 can be explained using resonance Raman concepts. The arrows in Fig. 7 represent the positions for laser excitation lines at 800 nm (Ti-:sapphire), 632.8 nm (He-Ne), and 514.5 nm (Ar^+). Figure 7 indicates that it is possible to be in resonance in the anti-Stokes side ($K^{-1}<1$) when 800 nm excitation is used and to be in resonance in the Stokes side ($K^{-1}>1$) when the experiment is performed using the other laser lines (as observed in Fig. 5). The same parameters used in Fig. 7 ($\bar{\nu}_{\mathrm{elec}}=13300\ \mathrm{cm}^{-1}$ and $\Gamma=1600\ \mathrm{cm}^{-1}$) can reproduce the observed dependence of K^{-1} ratio on vibrational energy for py adsorbed on silver (Fig. 5), as illustrated in Fig. 8.

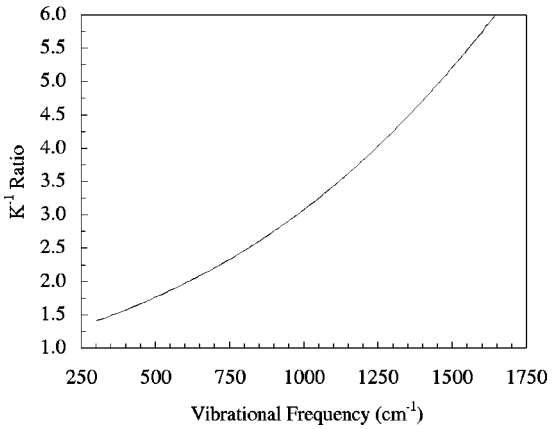

FIG. 8. Dependence of K^{-1} on the frequency of the vibrational band being measured, calculated for excitation at 632.8 nm.

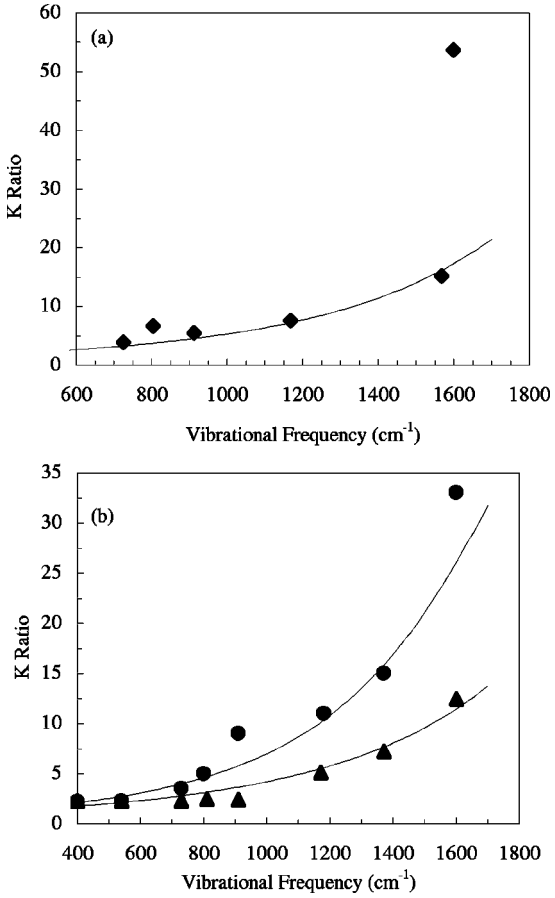

FIG. 9. Data points from (a) Kneipp *et al.* (Ref. 26) and (b) Haslett *et al.* (Ref. 25), showing the measured dependence of K on the frequency of the vibrational band being measured. Data points in (a) collected with 830 nm excitation. Circle data points in (b) collected with 780 nm excitation while triangle data points collected with 830 nm excitation. The solid lines are resonance Raman model fits using (a) $\bar{\nu}_{\mathrm{elec}}=14\,400\ \mathrm{cm}^{-1}$ and $\Gamma=600\ \mathrm{cm}^{-1}$, and (b) $\bar{\nu}_{\mathrm{elec}}=14\,800\ \mathrm{cm}^{-1}$ and $\Gamma=600\ \mathrm{cm}^{-1}$.

The resonance Raman model suggested here can also be used in the interpretation of the results presented in Refs. 25 and 26. Experimental data reported in Ref. 25 and 26 for crystal violet adsorbed on silver colloids are plotted in Fig. 9. Theoretical curves, calculated using Eq. (2) (after the approximations discussed above), are also plotted against the wave number in Fig. 9. Again, the objective was not to obtain a rigorous quantitative account of the phenomenon, but to probe if the resonance model can be used to fit the experimental data. The results presented in Ref. 26 are shown in

Fig. 9(a), and agree well with the model for all frequencies, except the highest observed vibrational energy. An electronic transition at 14400 cm^{-1} was used for the calculation. Results for the same system, obtained with two different excitation energies in Ref. 25, are plotted in Fig. 9(b). These also agreed well with the calculated curve, based on an electronic transition at 14 800 cm^{-1}. A damping factor of 600 cm^{-1} was used for all the calculated curves presented in Fig. 9. According to this model, the *K* ratios reported in Refs. 25 and 26 can be interpreted as a localized (narrow electronic band) resonance in the anti-Stokes region.

The *K* ratio for the vibrational mode at ca 1610 cm^{-1} in Fig. 9(a) is much higher than expected from the resonance model proposed here. Haslett *et al.* have demonstrated an increase in *K* ratio with the increase of laser power density.[25] In fact, *K* ratios increased significantly when the experiment was conducted above the threshold for photodecomposition.[25] It was suggested that the effect of the laser power on *K* could be related to photobleaching of the sample. Photobleaching of individual R6G molecules is much more efficient when the laser excitation energy is within the free molecule resonance, i.e., for R6G this photodecomposition would not occur for red or near IR excitations.[43] It is well established, however, that at high powers the incident radiation has a direct effect on the SERS intensity, independent of the incident wavelength, or the nature or chemical composition of the substrate.[44] No mechanism that would explain the increase in *K* ratio at these decomposing laser powers was indicated in Ref. 25. We suggest that the increase in *K* ratio with laser power and the excessively large *K* observed for high-energy vibrational modes may be attributed to the fact that the previously mentioned approximations on Eq. (2) are not appropriate under these extreme conditions.

One of the implicit assumptions used to determine *K* ratios is that the temperature on the surface is the same as the temperature of the liquid used as a reference [according to Eq. (1)]. However, the photodecomposition observed even with nonresonant laser excitation suggests that the temperature of the metal substrate may change significantly. A temperature increase is more probable in Raman microscopy experiments due to the tight focus conditions that create high power densities. The temperature changes should be related to the absorption of the substrate-molecule system, the reflectivity of the metal, and the rate of dissipation of the local energy. Water is not a good heat sink, but metals are well known to dissipate heat relatively quickly. Nevertheless, this process may be more limited in a colloidal substrate of nanometric size.

In order to estimate the temperature change caused by laser-induced heating, simple models of an electrode and a colloid were constructed based on standard heat transfer calculations.[45,46] In the case of an electrode, the area illuminated by the laser is only a small fraction of the total area, implying that it is reasonable to approximate the electrode as a semi-infinite slab. Since silver is a much better conductor of heat than the surrounding water, heat loss through the water is ignored in this case. In the case of the colloid, the model consists of a 100 nm silver sphere suspended in nonconvective water with the assumption of a constant temperature over the surface of the sphere. In both models the heat source is an 800 nm laser with a 2 μm diameter Gaussian-profile beam and a peak intensity of 5×10^{24} photons cm^{-2} s^{-1}, as used in Ref. 26, and an absorption coefficient of 25% is assumed. Under these conditions the models predict an increase in surface temperature of $\approx$10 K for the electrode and $\approx$70 K for the colloid. This is similar to the temperature of a silver colloidal particle considered in Ref. 26 and is not sufficient to cause morphological changes to the surface, as can be achieved with high-energy laser pulses.[48]

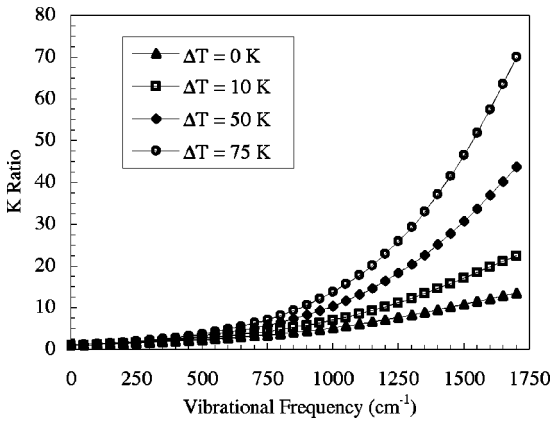

FIG. 10. Theoretical plots of Eq. (2) for $T_{UR}=298$ K and $T_{SERS}=T_{UR}+0$, 10, 50, and 75 K, assuming an 800 nm excitation source, an electronic band at 14 400 cm^{-1}, and a damping factor of 1000 cm^{-1}.

The expected bias on the experimentally determined *K* ratio due to a temperature difference between the substrate and the reference liquid can be evaluated using Eq. (2). Figure 10 shows theoretical plots of Eq. (2) with a fixed $T_{UR}=298$ K and varying values of T_{SERS}. The curves in Fig. 10 were calculated using an 800 nm excitation, an electronic band at 14 400 cm^{-1}, and a damping factor of 1000 cm^{-1}. The plots show the multiplicative effect of the temperature factor on the *K* ratios obtained under resonant conditions. Since the ratio between the Boltzmann factors follows an exponential law, increasing for higher vibrational energy, the differences between T_{UR} and T_{SERS} provoke a significant increase in the *K* ratios of the high-energy modes. This may explain why a damping factor of only 600 cm^{-1} (which is unusually narrow for an electronic transition) is required to fit the data in Fig. 9. Consequently, this effect causes a positive bias for the measured *K* ratios. Considering a band at 1600 cm^{-1}, Fig. 10 shows that this bias ranges from a factor of ca 2 for a 10 K difference between the temperature at the surface and the reference liquid to a factor of ca. 5 for T_{SERS} 75 K higher than the reference temperature.

According to our estimations, the laser-induced temperature changes are not as significant for molecules adsorbed on electrode surfaces as for species adsorbed on colloidal particles due to differences in dissipation to the bulk metal. Moreover, the temperature increase for a silver electrode illuminated under the conditions of our experiments (power densities around 10^{22} photons cm^{-2} s^{-1}) would be very

small. Therefore, we suggest that this effect does not significantly affect our results presented in Figs. 4–6. It is also plausible that the temperature increase depends on the new resonances present in the SERS system and may, therefore, be a molecule-dependent and excitation energy-dependent effect.

The resonance Raman model applied to SERS can explain the dependence of K on the excitation energy and on the vibrational energy.[25,26] However, it should also be noted that the resonance model used here [Eq. (2)] to explain the K ratios obtained in SERS experiments is independent of the origin of the resonance (the main parameters are the energy and the width of the resonance) and does not need to be the result of a dominant mechanism. A new methodology for the theoretical evaluation of the EM enhancement factor from molecules adsorbed on metal particle aggregates has been recently reported.[17] The model predicts molecular-specific resonant behavior with a relatively narrow bandwidth (the molecule is treated at an *ab initio* level in this case).[17] The theoretical model presented in Ref. 17 suggests a resonance in the near IR for py adsorbed on Ag colloids, this would lead to a preferential enhancement of the anti-Stokes for experiments using near IR excitation ($K>1$) and an enhancement of the Stokes signal for experiments using visible excitation ($K^{-1}>1$). In fact, a simple calculation using the model proposed in Ref. 17 yields K ratios of 0.92, 0.89, 4.2, and 5.0 for experiments using laser excitations at 514.5, 632.8, 780, and 830 nm, respectively.[47] These values are in good agreement with Figs. 5 and 7.

This work shows that a preferential enhancement of Stokes or anti-Stokes scattering can be explained using a resonance model without relying on optical pumping, and this model can be applied regardless of the origin of the resonance (CT or EM). The data presented here were obtained under different experimental conditions than the ones in Ref. 26, and differential enhancement of both Stokes and anti-Stokes were observed for a number of different systems. This indicates that this phenomenon is not specific to a given substrate (Ag colloids) nor limited to the conditions of single-molecule detection. Moreover, the power densities used in this work were of the order of 10^{22} photons cm^{-2} s^{-1}, which are around two to three orders of magnitude lower than used in the experiments reported in Ref. 26. This implies that an interpretation of our results for R6G based on the optical pumping mechanism would yield SERS cross sections 100 times bigger than the ones reported in Ref. 26. Another experimental result that has been linked to the supposed SERS-induced optical pumping is the nonlinear (quadratic) relationship between anti-Stokes intensity and the incident laser power.[26] Other authors have also observed a change in anti-Stokes intensity with laser power, but with a linear relationship.[25] However, it is clear that changes in laser power affect the anti-Stokes/Stokes ratio, but this effect can be attributed to temperature variation (as shown in Fig. 10), changes in the structure of the substrate, thermal-induced desorption/adsorption, and photodecomposition.[44]

In addition to the suggestion that SERS-induced vibrational pumping contradicts the current understanding of the SERS mechanism,[25] this concept also seems to violate some well-known results from the dynamics of vibrationally excited states in condensed matter. The vibration relaxation for molecules in solution is known to occur in several steps.[49,50,42] Immediately after photoexcitation the excess vibrational energy is localized in a specific vibrational mode. The vibrational energy is then redistributed to other internal modes in a process known as intramolecular vibrational redistribution (IVR). IVR occurs in subpicosecond time for large molecules and leads to a uniform vibrational temperature among all vibrational modes.[42,50] Vibrational cooling through the dissipation of the excess energy to the solvent molecules then occurs over ca 10 ps. The presence of the surface provides several additional channels for the relaxation of the excess vibrational energy.[51,52] Low-frequency molecular vibrations can couple directly with surface modes. In fact, vibrational relaxation through phonon modes is the main relaxation channel for molecules adsorbed on dielectric material.[51] However, quanta of vibrational energy can be transferred from the adsorbate to the conduction electrons of metals via electron-hole pairs.[52] This mechanism dominates for high-frequency modes, further reducing the lifetimes for the excited adsorbate molecules. Considering all the possible deexcitation pathways described above, it is unlikely that the vibrational energy in a dye molecule such as R6G will be localized for an appreciable length of time, which is another argument against the optical pumping mechanism as a possible cause for the anti-Stokes enhancement.

IV. CONCLUSIONS

K ratios for molecules adsorbed on a silver electrode were obtained. The dependence of the K ratios on the applied potential bias, the excitation wavelength, and the vibrational energy were explained using established SERS theories (CT and EM). K ratios different than unity were observed for all molecules adsorbed on silver. This may be an indication that a CT complex between the SERS substrate and the molecule was always formed. The position of the CT band of this complex relative to the energy of the Raman-shifted photon determines if a resonance occurs in the Stokes or the anti-Stokes region for a given excitation energy. A resonance Raman model was then applied to calculate the expected dependence on excitation and vibrational energy. Good agreement was observed between this resonance, Raman model, and the experimental data presented here and also with previous results reported in the literature. Resonances based on an EM model were also discussed. It is clear that processes operating under these resonance conditions would also explain the K ratios reported here. It was suggested that the laser-induced heating of the surface during a SERS experiment performed using high incident power densities can have a significant effect on the K ratios for molecules adsorbed on colloids. This effect yields unusually high K ratios, mainly for modes with high vibrational energy.

Finally, it was not necessary to invoke the previously proposed SERS-induced vibrational optical pumping model to explain any of the features observed here (and reported in the literature). The SERS-induced optical pumping would be an exciting phenomenon, but it is not required since all experi-

mental features related to the surface-enhanced anti-Stokes/Stokes ratio can be explained using current SERS theories. It is our conclusion that the extraordinary claim that optical pumping plays a very significant role in the determination of the *K* ratios for experiments performed under SERS conditions needs more experimental support to be considered as a viable explanation for this effect.

ACKNOWLEDGMENTS

This work was supported by grants from the University of Victoria (Start Up grant), the Canada Foundation for Innovation (CFI) and the British Columbia Knowledge and Development Fund (BCKDF). We also thank Dr. Donald E. Irish for the donation of the Raman equipment.

*Corresponding author. Email address: agbrolo@uvic.ca

[1] S. Nie and S.R. Emory, Science **275**, 1102 (1997).
[2] K. Kneipp, Y. Wang, H. Kneipp, L.T. Perelman, I. Itzkan, R.R. Dasari, and M.S. Feld, Phys. Rev. Lett. **78**, 1667 (1997).
[3] H. Xu, J. Aizpurua, M. Kall, and P. Apell, Phys. Rev. E **62**, 4318 (2000).
[4] K. Kneipp, H. Kneipp, I. Itzkan, R.R. Dasari, and M.S. Feld, Chem. Rev. (Washington, D.C.) **99**, 2957 (1999).
[5] A.M. Michaels, M. Nirmal, and L.E. Brus, J. Am. Chem. Soc. **121**, 9932 (1999).
[6] H.X. Xu, E.J. Bjerneld, M. Kall, and L. Borjesson, Phys. Rev. Lett. **83**, 4357 (1999).
[7] C. Eggeling, J. Schaffer, C.A.M. Seidel, J. Korte, G. Brehm, S. Schneider, and W. Schrof, J. Phys. Chem. A **105**, 3673 (2001).
[8] C.J.L. Constantino, T. Lemma, P.A. Antunes, and R. Aroca, Anal. Chem. **73**, 3674 (2001).
[9] A. Weiss and G. Haran, J. Phys. Chem. B **105**, 12 348 (2001).
[10] P. Hildebrandt and M. Stockburger, J. Phys. Chem. **88**, 5945 (1984).
[11] B. Pettinger, K. Krischer, and G. Ertl, Chem. Phys. Lett. **151**, 151 (1988).
[12] K. Kneipp, H. Kneipp, V.B. Kartha, R. Manoharan, G. Deinum, I. Itzkan, R.R. Dasari, and M.S. Feld, Phys. Rev. E **57**, R6281 (1998).
[13] E.J. Bjerneld, Z. Foldes-Papp, M. Kall, and R. Rigler, J. Phys. Chem. B **106**, 1213 (2002).
[14] T. Lemma and R.F. Aroca, J. Raman Spectrosc. **33**, 197 (2002).
[15] J.T. Krug, II, G.D. Wang, S.R. Emory, and S. Nie, J. Am. Chem. Soc. **121**, 9208 (1999).
[16] K.A. Bosnick, J. Jiang, and L.E. Brus, J. Phys. Chem. B **106**, 8096 (2002).
[17] S. Corni and J. Tomasi, J. Chem. Phys. **116**, 1156 (2002).
[18] A.M. Polubotko, J. Opt. A, Pure Appl. Opt. **1**, L18 (1999).
[19] A. Otto, Phys. Status Solidi A **188**, 1455 (2001).
[20] A. Otto, J. Raman Spectrosc. **33**, 593 (2002).
[21] M. Moskovits, Rev. Mod. Phys. **57**, 783 (1985).
[22] W.E. Doering and S. Nie, J. Phys. Chem. **106**, 311 (2002).
[23] A. Otto, T. Bornemann, U. Erturk, I. Mrozek, and C. Pettenkofer, Surf. Sci. **210**, 363 (1989).
[24] N.B. Persson, Chem. Phys. Lett. **82**, 561 (1981).
[25] T.L. Haslett, L. Tay, and M. Moskovits, J. Chem. Phys. **113**, 1641 (2000).
[26] K. Kneipp, Y. Wang, H. Kneipp, I. Itzkan, R.R. Dasari, and M.S. Feld, Phys. Rev. Lett. **76**, 2444 (1996).
[27] K. Kneipp, H. Kneipp, I. Itzkan, R.R. Dasari, and M.S. Feld, J. Phys.: Condens. Matter **14**, R597 (2002).
[28] A.G. Brolo, D.E. Irish, and B.D. Smith, J. Mol. Spectrosc. **405**, 29 (1997).
[29] J. Pemberton and M.M. Girand, J. Electroanal. Chem. **217**, 79 (1987).
[30] D.D. Tuschel, J.E. Pemberton, and J.E. Cook, Langmuir **2**, 380 (1986).
[31] A.G. Brolo and D.E. Irish, J. Electroanal. Chem. **414**, 183 (1996).
[32] S. Schneider, H. Grau, P. Halbig, P. Freunscht, and U. Nikel, J. Raman Spectrosc. **27**, 57 (1996).
[33] G. Li, H. Li, Y. Mo, X. Huang, and L. Chen, Chem. Phys. Lett. **330**, 249 (2000).
[34] A. Kudelski, J. Bukowska, and K. Jackowska, J. Raman Spectrosc. **25**, 153 (1994).
[35] D.J. Rogers, S.D. Luck, D.E. Irish, D.A. Guzonas, and G.F. Atkinson, J. Electroanal. Chem. **167**, 237 (1984).
[36] J.C. Rubin, P. Corio, M.C.C. Ribeiro, and M. Matz, J. Phys. Chem. **99**, 15765 (1995).
[37] A.G. Brolo, D.E. Irish, and J. Lipkowski, J. Phys. Chem. B **101**, 3906 (1997).
[38] J.S. Gao and Z.Q. Tian, Chem. Phys. Lett. **262**, 151 (1996).
[39] V.V. Marinyuk, R.M. Lazorenko-Manevich, and Y.M. Kolotyrkin, J. Electroanal. Chem. **110**, 111 (1980).
[40] J.R. Lombardi, R.L. Birke, T. Lu, and J. Xu, J. Chem. Phys. **84**, 4174 (1986).
[41] J. Thietke, J. Billmann, and A. Otto, in *Dynamics on Surfaces*, edited by B. Pullman (Reidel, New York, 1984), pp. 345–364.
[42] H. Okamoto, T. Nakabayashi, and M. Tasumi, J. Raman Spectrosc. **31**, 305 (2000).
[43] R.C. Maher, L.F. Cohen, and P. Etchegoin, Chem. Phys. Lett. **352**, 378 (2002).
[44] C. Viets and W. Hill, J. Phys. Chem. B **105**, 6330 (2001).
[45] K. C. Rolle, *Heat and Mass Transfer* (Prentice-Hall, Englewood Cliffs, NJ, 2000).
[46] J. F. Ready, *Effects of High-Power Laser Radiation* (Academic Press, New York, 1971).
[47] S. Corni (private communication).
[48] V.P. Safonov, V.M. Shalaev, V.A. Markel, Yu.E. Danilova, N.N. Lepeshkin, W. Kim, S.G. Rautian, and R.L. Armstrong, Phys. Rev. Lett. **80**, 1102 (1998).
[49] T. Nakabayashi, H. Okamoto, and M. Tasumi, J. Phys. Chem. B **101**, 7189 (1997).
[50] T. Nakabayashi, H. Okamoto, and M. Tasumi, J. Phys. Chem. A **102**, 9686 (1998).
[51] C.T. Rettner, D.J. Auerbach, J.C. Tully, and A.W. Kleyn, J. Phys. Chem. **100**, 13021 (1996).
[52] J.C. Tully, Annu. Rev. Phys. Chem. **51**, 153 (2000).